Development of an Efficient Geometry Optimization Method for Water Clusters

Hiroshi Takeuchi*

Division of Chemistry, Graduate School of Science, Hokkaido University, Sapporo 060-0810, Japan

Received July 15, 2008

A geometry optimization method for water clusters $(H_2O)_n$ was developed in the present study. The method was applied to the TIP3P and TIP4P water clusters in the range of $n \leq 30$, and the resulting structures were compared with the global-minimum structures in the literature ($n \leq 25$ for the TIP3P potential and $n \leq 30$ for the TIP4P potential). The method failed to reproduce the previously reported global minimum of the $n = 24$ TIP4P cluster. However, it was possible to find new global minima for the $n = 24$, 26−30 TIP3P cluster and the TIP4P clusters of 25, 28, 29, and 30 molecules.

INTRODUCTION

Geometry optimization of atomic/molecular clusters is a difficult problem in computational chemistry,[1] and the difficulty arises from two sources: theoretical level used in evaluation of cluster energies and strategy for searching optimal geometries of clusters. The choice of theoretical level depends on a tradeoff between precision and computational costs required for the optimization. The strategy to efficiently move from a local minimum to the global minimum on the potential energy surface of a cluster is indispensable since the optimal geometry of a cluster must be searched from an enormous number of stable geometries. An efficient strategy is to use the basin transformation where a rugged potential energy surface is transformed into a staircase potential by using local optimization.[1,2] This transformation is very useful since it reduces the number of local minima without varying the position of the global minimum. Other transformations from a rugged potential energy surface to a smooth one are also used to search the global minimum.[3−5]

In optimization methods based on the basin transformation, cluster geometries are modified to move from a local minimum to another one. Therefore, optimization algorithms are classified according to the number of particles with perturbation: (1) the Monte Carlo algorithms[2,6] and molecular dynamics simulations[7,8] where all particles are perturbed and (2) algorithms such as the dynamic lattice searching method[9−11] where several particles are perturbable. The genetic algorithms,[12−15] the conformational space annealing method,[16] and the hierarchical optimization method[17] include both partial and overall structural changes of a cluster.

Efficiencies of algorithms in class (2) are affected by selection of perturbed particles and movement of selected particles. In the dynamic lattice searching method,[9,10] Shao and co-workers calculated the energy $E(i)$ of an atom i in the Lennard-Jones (LJ) atomic cluster consisting of n atoms as follows

$$E(i) = \sum_{j \neq i}^{n} E(i,j) \tag{1}$$

where $E(i, j)$ denotes the potential energy between the i-th and j-th atoms. According to the order of atom energies $E(i)$, the atoms are selected stepwise from the highest-energy atom. They are moved to the most stable lattice space (vacant site) on the surface of a cluster. In the simple greedy method with energy-based perturbation,[18] the selection probability of an atom i is proportional to $\exp(E(i)/T)$ where T is the temperature. The selected atom is moved to a position with the distance

$$R = \alpha^2 \left\{ 1 + \left(\frac{3n}{4\pi} \right)^{1/3} \sqrt[6]{2} \right\}$$

from the center of mass of a cluster where α is a random number between 0 and 1, and $\sqrt[6]{2}$ is an equilibrium distance between two LJ particles. In continuous extremal optimization,[19] each atom is ranked according to its energy $E(i)$, and an atom with the rank k is selected with the probability $P(k) \sim k^{-\tau}$ where τ is a predetermined value. The coordinates of the selected atom are randomly changed, and the above steps of selection and random movement are repeated several times. In an evolutionary optimization method,[20] a similar selection method is adopted, and selected atoms are moved to random positions on the surface of a cluster.

In genetic algorithms, Niesse and Mayne[12] created new geometries from one or two configurations by using genetic operators; inversion, N-point crossover, and 2-point crossover operators. Barrón et al.,[13] Deaven et al.,[14] and Hartke[15] used a crossover operator peculiar to clusters to generate new clusters from a pair of clusters: each configuration is cut into halves by a plane, and one of the halves of a configuration is exchanged for one of the halves of another configuration. To correct a cluster geometry slightly differing from the global-minimum geometry, Hartke[15] proposed the directed operator; it modifies a cluster geometry by moving the atom with the highest energy to the most stable vacant site.

The present author investigated an efficient algorithm for geometry optimization of LJ clusters.[21] In the method, the highest-energy group of m atoms is selected according to the following energy:

$$E(k_1, k_2, \cdots, k_m) = \sum_{i=1}^{m} E(k_i) - \sum_{i=1}^{m-1} \sum_{j=i+1}^{m} E(k_i, k_j) \tag{2}$$

Here, $E(k_1, k_2, ..., k_m)$ means the contribution of the m atoms (with atom numbering of $k_1, k_2, ...,$ and k_m) to the total energy

* Corresponding author e-mail: takehi@sci.hokudai.ac.jp.

10.1021/ci800238w CCC: $40.75
Published on Web 11/01/2008

Table 1. Previous Studies Where Geometry Optimization of Water Clusters $(H_2O)_n$ with $n \geq 10$ Was Performed

author(s)	empirical potential	cluster size n
Pillary, Olszewski, and Piela[33]	MCY	2−10
Tsai and Jordan[34]	TIP4P	8, 12, 16, 20
Sremaniak, Perera, and Berkowitz[35]	SPC/E, POL1	12, 16, 20
Nisse and Mayne[36]	TIP3P	2−13
Wales and Hodges[37]	TIP3P	2−13
	TIP4P	2−21
Qian, Stöckelmann, and Hentschke[38]	SPC/E	2−14
Hartke[39]	TIP4P	2−22
Guimarães, Belchior, Johnston, and Roberts[40]	TIP3P	2−13
	TIP4P	11−13
Kabrede and Hentscke[41]	SPC/E, TIP3P, TIP4P	2−25
Hartke[42]	TTM2-F	2−30
Kazimirski and Buch[43]	TIP4P, TTM2-R	20−22
James, Wales, and Hernández-Rojas[44]	TIP5P	2−21
Kabrede[45]	TIP4P	25−30
Bandow and Hartke[46]	TTM2-F	4−34

of the cluster. It should be noted that the sum of $\sum_{i=1}^{m} E(k_i)$ is not exact for the potential energy of the m atoms since the energy of $E(k_i, k_j)$ $(j \neq i)$ is doubly evaluated in the sum.

Subsequently to atom selection, the interior and surface operators are used. These operators move the selected atoms to the interior of the cluster and to the most stable positions on the cluster surface, respectively. The surface operator with one atom is identical to the directed operator.[15] Since one to four atoms are moved by the surface operator as described later, it explores a wider region on the potential energy surface than the directed operator.

The above method yielded putative global minima for LJ_{10} to LJ_{561} reported in the literature[2,5,13,22,23] with reducing computational effort compared with previous unbiased methods.[9,17,18,20,24] In addition, it was possible to locate new global minima for LJ_{506}, LJ_{521}, LJ_{536}, LJ_{537}, LJ_{538}, and LJ_{541}. Therefore, the proposed method is considered to be excellent.

To treat a more complicated problem, geometry optimization of clusters of nonspherical molecules, the above method was modified.[25] By using the modified method, geometries of benzene clusters $(C_6H_6)_n$ with $n \leq 30$ were optimized. Compared with the global minima reported in the literature,[26−31] it was found that the method located new global minima for $(C_6H_6)_{11}$, $(C_6H_6)_{14}$, and $(C_6H_6)_{15}$. Moreover, putative global minima for $(C_6H_6)_{16}$ to $(C_6H_6)_{30}$ were first reported.

Recently the method was applied to the geometry optimization of $(CO_2)_n$ in the range of $n \leq 40$.[32] The method improved global minima for $(CO_2)_n$, $n = 23$, 25, 35, and

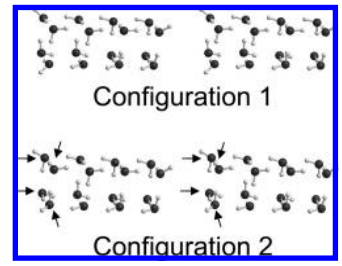

Figure 1. Stereographic views of two configurations of $(H_2O)_{16}$. Differences between the two structures are indicated by arrows. Configuration 1 corresponds to the global minimum of the $n = 16$ TIP4P cluster.

global minima of many clusters under investigation were first proposed. In the present study, water clusters $(H_2O)_n$ were chosen as a target. Water clusters have been investigated by calculations at several levels.[33−70] The present author confines his attention to calculations with empirical potentials because of their low computational costs. Many investigations on global optimization of $(H_2O)_n$ for $n \geq 10$ have been performed employing empirical potentials[33−46] as summarized in Table 1. The TIP3P and TIP4P potentials[71] have been widely used in the geometry optimization. Therefore, the above optimization method was preliminarily applied to the TIP3P and TIP4P clusters with up to 19 molecules. The results of the calculations showed that many local-minimum configurations similar to the global-minimum configuration were searched. Figure 1 shows a typical result obtained in the geometry optimization of $(H_2O)_{16}$. Differences between these configurations are seen in the directions of hydrogen bonds in the four-membered ring. Configuration 2 is easily converted into configuration 1 if the directions of the four hydrogen bonds in the ring are reversed. In the present study, therefore, an operator reversing the directions of hydrogen bonds simultaneously is introduced in the above method to construct a new optimization method. The details of the new method are explained below.

GEOMETRY OPTIMIZATION

TIP3P and TIP4P Potentials. The potential energy of $(H_2O)_n$ takes the form:[71]

$$E_n = \sum_{i=1}^{n-1} \sum_{j=i+1}^{n} E(i,j) = \sum_{i=1}^{n-1} \sum_{j=i+1}^{n} \left[\frac{C_{12}}{(r_{ij}^{OO})^{12}} - \frac{C_6}{(r_{ij}^{OO})^6} + \sum_{k=1}^{3} \sum_{l=1}^{3} \frac{q_k q_l e^2}{r_{ij}^{kl}} \right] \quad (3)$$

Here k and l represent sites of electronic charges in the two molecules i and j, respectively, and r_{ij}^{OO} and r_{ij}^{kl} denote the O...O distance between the molecules i and j and the distance between the two sites k and l, respectively. The potential parameters, C_{12}, C_6, and q, and geometrical information on water molecule are summarized in Table 2.

Optimization Algorithm. The algorithm proposed in the present study repeats the cycle shown in Figure 2 where interior (I), surface (S), orientation (O), and hydrogen-bond-arrangement (H) operators optimize a cluster geometry by trial and error. A cycle begins from generating an initial cluster geometry; water molecules are randomly placed in a sphere having a radius of $R = (3n/4\pi)^{1/3} r_e$ where r_e denotes the equilibrium distance between two molecules. It is

Table 2. Parameters of the TIP3P and TIP4P Potentials Used in the Present Study

parameter	TIP4P	TIP3P
r(O−H)/Å	0.9572	0.9572
∠HOH/°	104.52	104.52
$C_{12}{}^a$/kJ Å^{12} mol^{-1}	2.510400× 10^6	2.435088 × 10^6
$C_6{}^a$/kJ Å^6 mol^{-1}	2552.24	2489.48
q_H/e	0.520	0.417
r(O-M)/Å	0.15	0.0

[a] Values are taken from ref 68, whereas the original values[71] are given in kcal mol^{-1}.

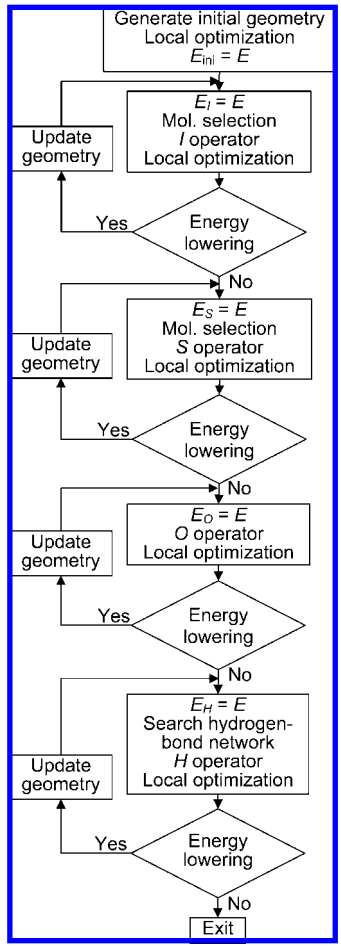

Figure 2. The optimization cycle proposed for water clusters.

assumed to be 2.75 Å, a value of the O...O distance of the TIP4P water dimer.[44] The initial geometry is locally optimized by using a quasi-Newton method (the L-BFGS[72] method) and then modified by using *I*, *S*, *O*, and *H* operators in that order.

The highest-energy group consisting of *m* outer molecules is selected according to eq 2 where *m* is a variable as described below. The selected molecules are moved by the *I* and *S* operators. The *I* operator gives a perturbation on a cluster configuration by moving the molecules on the surface of the sphere whose center coincides with the oxygen-atom position of the molecule closest to center of mass of the cluster. The radius of the sphere is fixed at $r_e/2$. Orientations of the moved molecules are randomly determined. The number of *m* is randomly selected from 1 to 5.[25] Modified geometries are locally optimized by means of the L-BFGS[72] method.

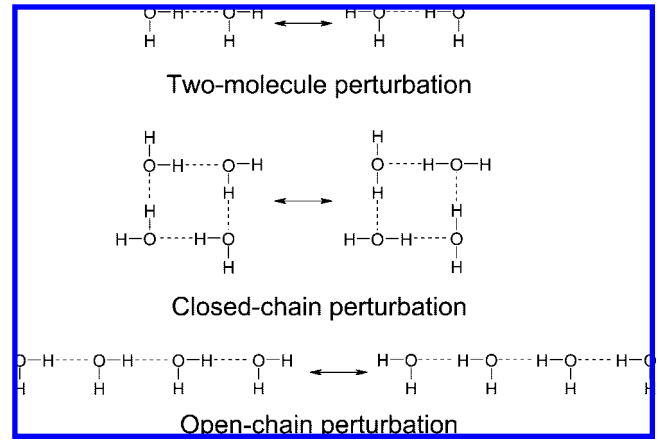

Figure 3. Perturbations of hydrogen-bond networks.

If the energy of a cluster is not improved during the last 100 local optimizations, calculation proceeds to the next step where the *S* operator is applied to clusters. Otherwise, the geometry is updated and the *I* operator is repeated. The best performance of the *I* operator for water clusters was obtained with this procedure.

In the *S* operator,[25] the first step is to search stable positions on the surface of the template cluster prepared by removing the *m* selected molecules from a cluster. Then for all the combinations of *m* stable positions, the energy $E_{surface}$ of these positions is calculated by

$$E_{surface}(S_1, S_2, \cdots, S_m) = \sum_{i=1}^{m} E_{template}(S_i) + \sum_{i=1}^{m-1} \sum_{j=i+1}^{m} E(S_i, S_j) \quad (4)$$

where the *m* positions are represented by S_1, S_2,..., S_m, and $E_{template}(S_i)$ denotes a potential energy between a molecule in a position S_i and the template cluster. The lowest potential energy $E_{surface}^{min}$ is derived from all the combinations. In the cases with $m \geq 2$, for the combinations with energies less than $E_{surface}^{min} + 5.0$ kJ mol^{-1}, the positions are simultaneously optimized.[25] The molecules removed in the first step are moved to the positions giving the lowest energy. The geometry generated by the *S* operator is optimized by means of the L-BFGS[72] method.

The number *m* is initially set at 1. It increases to 4 at an interval of 1 when the energy of a cluster is not lowered by using this operator.[21,25] If the energy is improved, the cluster geometry is updated and *m* is again set at 1. In the *S* operator with $m = 1$, the highest-energy molecule, the second highest-energy molecule, and the third highest-energy molecule are selected in that order.[21,25]

The *O* operator randomizes orientational degrees of freedom of all the molecules in a cluster. The resulting geometries are optimized by means of the L-BFGS[72] method. Modification of orientational degrees of freedom of molecules was carried out in previous studies on water clusters[37,44,46] and nitrogen clusters.[73] If the energy of a cluster is not lowered during the last 100 local optimizations, the *H* operator is performed.

The *H* operator modifies hydrogen-bond networks as shown in Figure 3 and keeps the number of hydrogen bonds in the networks. For two molecules sharing a hydrogen bond, the orientations of the molecules are changed if the hydrogen bonds next to the two molecules are kept. For more than

Table 3. Number of Repeated Cycles (N_r) in Geometry Optimization of $(H_2O)_n$ and the Number of Cycles (N_s) Which Locate the Same Lowest-Energy Configuration

	TIP3P		TIP4P			TIP3P		TIP4P	
n	N_r	N_s	N_r	N_s	n	N_r	N_s	N_r	N_s
2[a]	100	53	100	60	17	1000	14	1000	11
3[a]	100	61	100	57	18	3000	2	3000	5
4[a]	100	65	100	81	19	1000	3	2000	44
5[a]	100	20	100	12	20	5000	12	5000	4
6[a]	100	21	100	6	21	5000	8	5000	3
7	100	98	100	100	22	10000	5	65000	2
8	100	100	100	94	23	20000	12	10000	6
9	100	100	100	99	24	50000	4	300000	11[b]
10	100	15	100	89	25	20000	2	40000	5
11	100	65	100	21	26	70000	7	160000	1
12	100	13	100	52	27	130000	2	250000	1
13	100	30	100	30	28	160000	2	240000	1
14	100	16	100	44	29	140000	2	140000	2
15	100	5	100	7	30	590000	1	230000	1
16	1000	10	3000	6					

[a] Random search method is used. [b] The global minimum reported by Kabrede and Hentschke[41] could not be searched. The value means the number of the cycles where the local minimum with the energy of −1063.258 kJ mol^{-1} was searched.

Table 4. Lowest-Energy Values of $(H_2O)_n$ Obtained in the Present Study (in kJ mol^{-1})

n	TIP3P	TIP4P	n	TIP3P	TIP4P
2	−27.363	−26.088	17	−713.616	−723.809
3	−72.970	−69.994	18	−764.710	−773.233
4	−122.563	−116.591	19	−810.467	−821.038
5	−162.147	−152.109	20	−859.306	−872.990
6	−199.953	−197.781	21	−906.870	−916.706
7	−242.332	−243.573	22	−954.896	−966.622
8	−295.603	−305.519	23	−1005.083	−1015.599
9	−341.540	−344.436	24	−1052.068	−1063.258
10	−386.775	−391.023	25	−1103.576	−1113.037
11	−428.069	−431.490	26	−1147.327	−1160.674
12	−478.514	−492.909	27	−1197.558	−1211.164
13	−523.399	−532.972	28	−1247.620	−1259.932
14	−572.694	−582.992	29	−1302.027	−1306.864
15	−619.622	−628.373	30	−1342.658	−1361.223
16	−664.138	−681.194			

two molecules, there are two types of hydrogen-bond networks: open chains and closed chains. Two end molecules of an open chain may share hydrogen bonds with the water molecules next to the chain. In this case, the *H* operator affects the hydrogen bonds next to the chain. On the other hand, the *H* operator gives no effect on the hydrogen bonds next to closed chains. The number of open chains was larger than that of closed chains, but the energy-lowering due to modification of closed chains occurred more frequently than that due to modification of open chains. Therefore, the application of this operator was limited to closed chains (ring structures).

The number of molecules modified by the *H* operator is initially set at 2 and increases to 10 at an interval of 1. If the energy of the cluster perturbed by this operator is improved by a subsequent local optimization,[72] the geometry is updated and this operator is repeated with an initial condition of $m = 2$. Kazimirski and Buch[43] used a procedure similar to the *H* operator in their study on water clusters; open chains and closed chains were selected at random.

Geometry optimizations were executed in serial mode on a single processor, and nine processors were available for calculation. The lowest-energy structures of $(H_2O)_n$ for $n \leq 6$ were easily found by a random search method where many geometries randomly generated were optimized by means of the L-BFGS[72] method. The optimal geometries of clusters for $7 \leq n \leq 30$ were searched by repeating the cycle shown

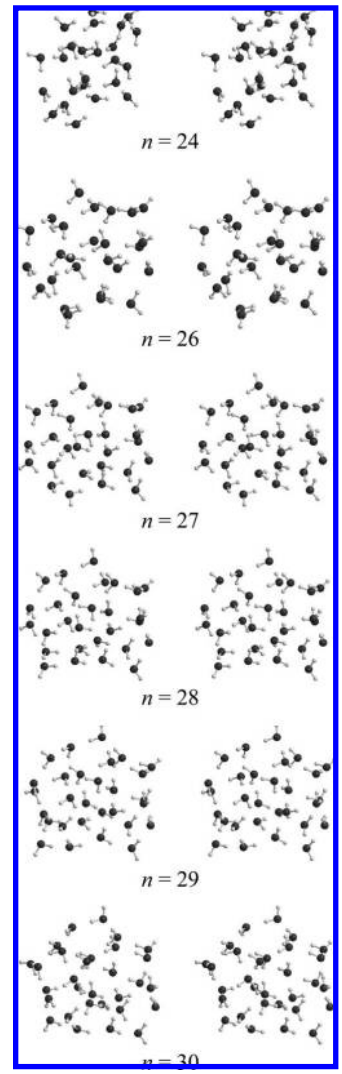

Figure 4. Stereographic views of new global minima of the TIP3P $(H_2O)_n$, $n = 24$, 26−30, clusters.

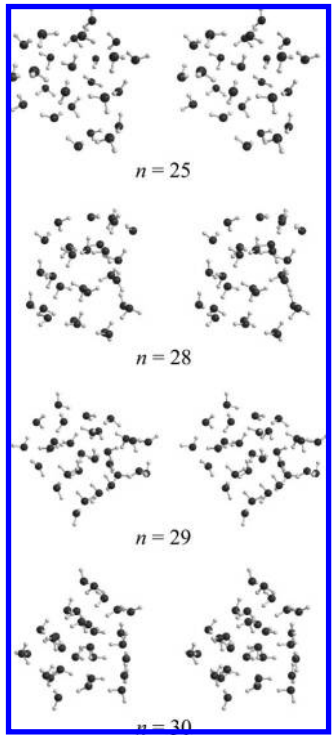

Figure 5. Stereographic views of new global minima of the TIP4P $(H_2O)_n$, $n = 25$, 28−30 clusters.

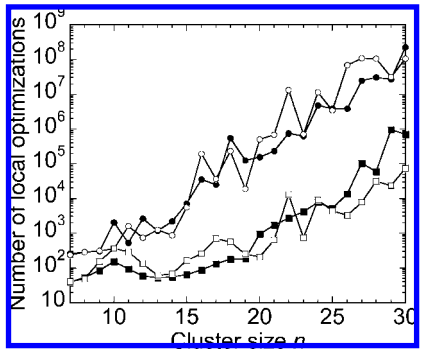

Figure 6. The number of local optimizations required for obtaining global minima of clusters: closed circles, TIP3P water clusters; open circles, TIP4P clusters; open squares, benzene clusters; closed squares, CO_2 clusters.

in Figure 2. For each cluster under investigation, the number of repeated cycles N_r is listed in Table 3 together with the number of cycles (N_s) yielding the same lowest-energy configuration. The average number of local optimizations N_c in a cycle was smaller than 460 for the clusters for $n \leq 30$. For the TIP4P clusters of 10, 20, and 30 molecules, a cycle took approximately 5, 27, and 74 s, respectively, on a 3 GHz Pentium IV processor. Table 4 lists the lowest-energy values obtained in the present study.

DISCUSSION

TIP3P Water Clusters. Global minima of the clusters for $n = 2-13$ were obtained by Nisse and Mayne.[36] Wales and Hodges[37] confirmed their results for $n = 2-10$ and revised the data for $n = 11-13$. The global minima for $n = 2-13$ were reproduced by Guimarães et al.[40] and by Kabrede and Hentschke.[41] The global-minimum energies reported in ref 37 agree with those in the present study within 0.001 kJ mol^{-1} (see Table S3 in the Supporting Information).

Kabrede and Hentschke[41] also reported global minima for $n = 14-25$. The differences between the energies of these clusters in ref 41 and the corresponding energies in Table 4 are less than 0.2 kJ mol^{-1} except for $(H_2O)_{24}$. The structures of the clusters for $n = 14-23$, 25 in ref 41 are in good agreement with the structures obtained in the present study. The calculated energy of $(H_2O)_{24}$ in the present study is 0.8 kJ mol^{-1} lower than that reported by Kabrede and Hentschke (−1051.3 kJ mol^{-1}).[41] Therefore, a new global minimum of the $n = 24$ cluster was found in the present study. The structure is shown in Figure 4. This cluster contains an interior molecule, whereas the previous configuration[41] takes a tube structure composed of four hexagonal rings.

The global minima of the clusters with the size of $26 \leq n \leq 30$ are first reported in this article. Figure 4 shows that there are two interior molecules in these clusters, whereas clusters with one or no interior molecule are obtained for clusters with the size of $n \leq 25$.[41]

TIP4P Water Clusters. The lowest energies of water clusters for $n \leq 21$ were reported by Wales and Hodges.[37] These values are equal to the lowest energies obtained in the present study within 0.002 kJ mol^{-1} (see Table S4 in the Supporting Information). Hartke[39] reproduced the above global minima and proposed a putative global-minimum structure for $n = 22$. Cluster geometries were optimized for $n \leq 25$ by Kabrede and Hentschke,[41] for $20 \leq n \leq 22$ by Kazimirski and Buch,[43] and for $25 \leq n \leq 30$ by Kabrede,[45] respectively. According to the previous studies, the energies of global minima for $n = 22-30$ are −966.418,[41] −1015.38,[41] −1064.75,[41] −1111.95,[45] −1160.67,[45] −1211.15,[45] −1258.18,[45] −1306.13,[45] and −1359.09[45] kJ mol^{-1}, respectively. The values for $n = 26$, 27 are in good agreement with the corresponding ones in Table 4. However, the energy of $(H_2O)_{24}$ obtained in the present study is higher than that by Kabrede and Hantschke[41] by 1.49 kJ mol^{-1}; positions of oxygen atoms in the geometry in ref 41 are different from those in the present study.

The 25-, 28-, 29-, and 30-molecule clusters are more stable than the clusters reported by Kabrede[45] by 1.09, 1.75, 0.73, and 2.13 kJ mol^{-1} in energy, respectively. These structures are shown in Figure 5. The $(H_2O)_{25}$ and $(H_2O)_{30}$ configurations obtained in the present study and those in ref 45 have approximately the same overall geometries for positions of O atoms. The differences between these configurations are found in the hydrogen-bond networks. The structural differences between the 28- and 29-molecule clusters obtained by the present method and those in the literature[45] are more pronounced since they have different geometries for positions of O atoms.

Similarities and differences between the TIP3P and TIP4P structures are discussed by Kabrede and Hentschke.[41] A more sophisticated model potential TTM2-F was used by Hartke.[42] The geometrical differences between the TIP4P and TTM2-F clusters in the range of $n \leq 22$ are found for $n = 13$, 17, 21, 22.

Efficiency of the Present Optimization Method. Figure 6 shows the average number of local optimizations (N_rN_c/N_s) required for searching the lowest-energy geometry of each cluster. The number of local optimizations for a TIP3P cluster is similar to that for the corresponding TIP4P cluster. This suggests that the number of local minima on the TIP3P potential energy surface is not significantly different from

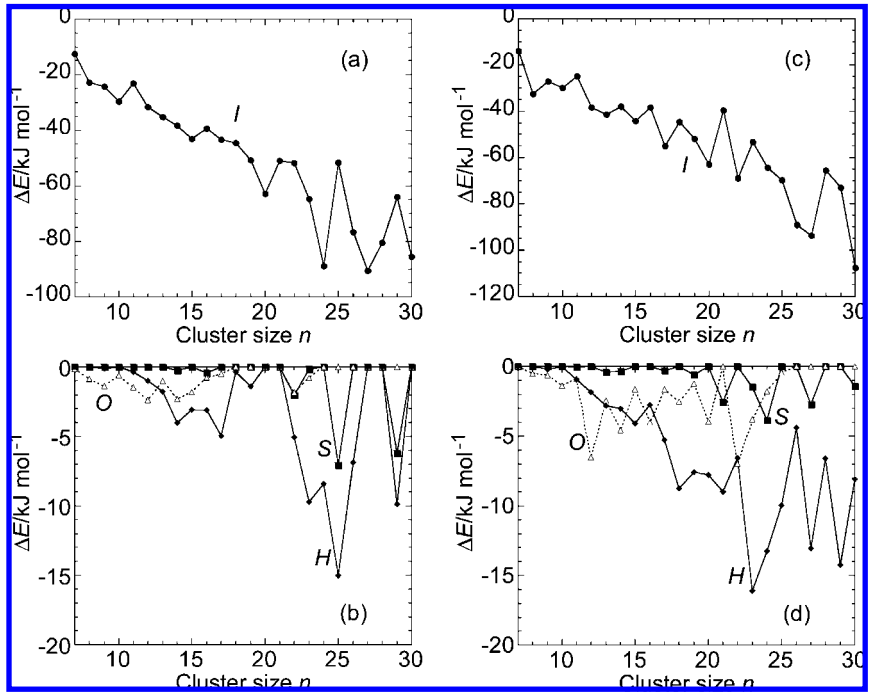

Figure 7. Energy lowering due to the *I*, *S*, *O*, and *H* operators: (a) $\Delta E = E_I - E_{ini}$ for the TIP3P potential; (b) the lines indicated by *S*, *O*, and *H* represent $E_S - E_I$, $E_O - E_S$, and $E_H - E_O$ for the TIP3P potential, respectively; (c) $\Delta E = E_I - E_{ini}$ for the TIP4P potential; and (d) the lines indicated by *S*, *O*, and *H* represent $E_S - E_I$, $E_O - E_S$, and $E_H - E_O$ for the TIP4P potential, respectively.

that on the TIP4P surface. Comparison of the number of local optimizations for $(H_2O)_n$ with the corresponding numbers for $(C_6H_6)_n$[25] and for $(CO_2)_n$[32] indicates that global optimization of water clusters is more difficult than that of benzene clusters and carbon dioxide clusters.

The number of local optimizations is approximately expressed by a formula of exp(0.63*n*). This suggests that 9×10^{10} local optimizations are required for searching the global minimum of $(H_2O)_{40}$. For this cluster, 100 local optimizations take ca. 30 s. Therefore, the time needed for searching the global minimum is estimated to be 3×10^5 days. More efficient algorithms must be developed to treat water clusters of 40 molecules.

To examine the efficiency of the geometrical operators, *I*, *S*, *O*, and *H*, in more detail, the energies of initial clusters and the lowest energies of clusters obtained by using the operations (E_{ini}, E_I, E_S, E_O, and E_H shown in Figure 2) were averaged over the cycles where the energies listed in Table 4 were obtained. The energy-lowering due to these operators is shown in Figure 7. The *I* operator considerably reduces energies of water clusters by 15 to 110 kJ mol^{-1}. The large energy changes induced by the *I* operator were previously found in the studies on LJ clusters,[21] benzene clusters,[25] and CO_2 clusters.[32] Therefore, the *I* operator combined with local optimization is considered to be excellent for improving cluster geometries.

The *S* operator gives no improvement for the following clusters: the $n = 7-13$, 15, 17−21, 24, 26−28, 30 TIP3P clusters and the $n = 7 - 10$, 12, 15, 16, 18, 20, 25, 26, 28, 29 TIP4P clusters. However, this operator efficiently lowered the energies of Lennard-Jones, benzene, and CO_2 clusters.[21,25,32] For example, the energies of the $n = 19$, 22−24, 26, 27, 29−40 $(CO_2)_n$ clusters were reduced by 8 to 24 kJ mol^{-1} by using the *S* operator.[32] This difference probably originates from hydrogen bonds in water clusters. Template clusters created in the first step of the *S* operator may be unstable because of removing some molecules in hydrogen-bond networks. Therefore, geometry optimization of template clusters can improve the efficiency of this operator.

The *O* operator is not efficient for the $n = 18-21$, 24−30 TIP3P clusters and the $n = 21$, 26−30 TIP4P clusters. This operator was not useful for geometry optimization of most of the $(CO_2)_n$ clusters for $19 \le n \le 40$. Therefore, the efficiency of the *O* operator is limited for relatively small molecular clusters.

For most of the water clusters, the *H* operator is more efficient than the *S* and *O* operators. The results obtained for relatively large clusters ($20 \le n \le 30$) showed that cluster energies were lowered by modifying hydrogen-bond networks consisting of 2, 4−10 molecules; for example, in a cycle yielding the global minimum of the $n = 23$ TIP4P cluster, geometrical perturbations on hydrogen-bond networks of 2, 4, 5, 6, 7, 8, and 9 molecules improved its energy. It should be noted that many perturbations due to the *H* operator are performed for a cycle and that most of the perturbations do not lower cluster energies. In addition, as described before, the *H* operator is not carried out for open-chain networks. Therefore, a lot of configurations with different hydrogen-bond networks and similar potential energies can be derived from variations of directions of hydrogen bonds. This must cause complexity of potential energy surfaces of water clusters.

CONCLUSION

The optimization method based on the basin transformation is proposed for searching optimal geometries of water clusters. The method improves global minima for the $n = 24$ TIP3P cluster and the $n = 25$, 28−30 TIP4P clusters and yields new global minima for the TIP3P water clusters for $26 \le n \le 30$. However, the global minimum of the $n = 24$

TIP4P cluster was not located by the present method; geometrical differences between the global minimum and the local minimum obtained in the present study were found for positions of O atoms. This problem may be solved by modifying the *S* operator since the operator introduces perturbations for oxygen-atom positions.

The interior operator is excellent for lowering potential energies of water clusters in accordance with the results obtained for Lennard-Jones atomic clusters, benzene clusters, and carbon dioxide clusters. The hydrogen-bond-arrangement operator is more efficient than the surface and orientation operators. The use of the interior and hydrogen-bond-arrangement operators is essential to the performance of the present method.

ACKNOWLEDGMENT

This work was supported by a Grant-in-Aid for Scientific Research (C) (19550001) from the Japan Society for Promotion Science (JSPS).

Supporting Information Available: Tables of Cartesian coordinates of the global minima and global-minimum energies obtained in the present study. This material is available free of charge via the Internet at http://pubs.acs.org.

REFERENCES AND NOTES

(1) Wales, D. J. Global Optimization. In Energy Landscapes; Cambridge University Press: Cambridge, 2003; pp 330−352.
(2) Wales, D. J.; Doye, J. P. K. Global Optimization by Basin-Hopping and the Lowest Energy Structures of Lennard-Jones Clusters Containing up to 110 Atoms. *J. Phys. Chem. A* **1997**, *101*, 5111–5116.
(3) Pillardy, J.; Liwo, A.; Scheraga, H. A. An Efficient Deformation-Based Global Optimization Method (Self-Consistent Basin-to-Deformed-Basin Mapping (SCBDBM)). Application to Lennard-Jones Atomic Clusters. *J. Phys. Chem. A* **1999**, *103*, 9370–9377.
(4) Pillardy, J.; Piela, L. Smoothing Techniques of Global Optimization: Distance Scaling Method in Searches for Most Stable Lennard-Jones Atomic Clusters. *J. Comput. Chem.* **1997**, *18*, 2040–2049.
(5) Shao, X.; Jiang, H.; Cai, W. Parallel Random Tunneling Algorithm for Structural Optimization of Lennard-Jones Clusters up to $N = 330$. *J. Chem. Inf. Comput. Sci.* **2004**, *44*, 193–199.
(6) Liu, H.; Jordan, K. D. Finite Temperature Properties of $(CO_2)_n$ Clusters. *J. Phys. Chem. A* **2003**, *107*, 5703–5709.
(7) Torchet, G.; de Feraudy, M.-F.; Boutin, A.; Fuchs, A. H. Structural Transformation in $(CO_2)_N$ Clusters, $N < 100$. *J. Chem. Phys.* **1996**, *105*, 3671–3678.
(8) Maillet, J.-B; Boutin, A.; Fuchs, A. H. From Molecular Clusters to Bulk Matter. II. Crossover from Icosahedral to Crystalline Structures in CO_2 Clusters. *J. Chem. Phys.* **1999**, *111*, 2095–2102.
(9) Shao, X.; Cheng, L.; Cai, W. A Dynamic Lattice Searching Method for Fast Optimization of Lennard-Jones Clusters. *J. Comput. Chem.* **2004**, *25*, 1693–1698.
(10) Yang, X.; Cai, W.; Shao, X. A Dynamic Lattice Searching Method with Constructed Core for Optimization of Large Lennard-Jones Clusters. *J. Comput. Chem.* **2007**, *28*, 1427–1433.
(11) Shao, X.; Yang, X.; Cai, W. A Dynamic Lattice Searching Method with Interior Operation for Unbiased Optimization of Large Lennard-Jones Clusters. *J. Comput. Chem.* **2008**, *29*, 1772–1779.
(12) Niesse, J. A.; Mayne, H. R. Global Geometry Optimization of Atomic Clusters Using a Modified Genetic Algorithm in Space-Fixed Coordinates. *J. Chem. Phys.* **1996**, *105*, 4700–4706.
(13) Barrón, C.; Gómez, S.; Romero, D.; Saavedra, A. A Genetic Algorithm for Lennard-Jones Atomic Clusters. *Appl. Math. Lett.* **1999**, *12*, 85–90.
(14) Deaven, D. M.; Tit, N.; Morris, J. R.; Ho, K. M. Structural Optimization of Lennard-Jones Clusters by a Genetic Algorithm. *Chem. Phys. Lett.* **1996**, *256*, 195–200.
(15) Hartke, B. Global Cluster Geometry Optimization by a Phenotype Algorithm with Niches: Location of Elusive Minima, and Low-Order Scaling with Cluster Size. *J. Comput. Chem.* **1999**, *20*, 1752–1759.
(16) Lee, J.; Lee, I.; Lee, J. Unbiased Global Optimization of Lennard-Jones Clusters for $N \leq 201$ Using the Conformational Space Annealing Method. *Phys. Rev. Lett.* **2003**, *91*, 080201-1–080201-4.
(17) Krivov, S. V. Hierarchical Global Optimization of Quasiseparable Systems: Application to Lennard-Jones Clusters. *Phys. Rev. E* **2002**, *66*, 025701-1–025701-4.
(18) Cheng, L.; Cai, W.; Shao, X. An Energy-Based Perturbation and a Taboo Strategy for Improving the Searching Ability of Stochastic Structural Optimization Methods. *Chem. Phys. Lett.* **2005**, *404*, 182–186.
(19) Zhou, T.; Bai, W.; Cheng, L.; Wang, B. Continuous Extremal Optimization for Lennard-Jones Clusters. *Phys. Rev. E* **2005**, *72*, 016702-1–016702-5.
(20) Cheng, L.; Cai, W.; Shao, X. A Connectivity Table for Cluster Similarity Checking in the Evolutionary Optimization Method. *Chem. Phys. Lett.* **2004**, *389*, 309–314.
(21) Takeuchi, H. Clever and Efficient Method for Searching Optimal Geometries of Lennard-Jones Clusters. *J. Chem. Inf. Model.* **2006**, *46*, 2066–2070.
(22) Romero, D.; Barrón, C.; Gómez, S. The Optimal Geometry of Lennard-Jones Clusters: 148−309. *Comput. Phys. Commun.* **1999**, *123*, 87–96.
(23) Xiang, Y.; Jiang, H.; Cai, W.; Shao, X. An Efficient Method Based on Lattice Construction and the Genetic Algorithm for Optimization of Large Lennard-Jones Clusters. *J. Phys. Chem. A* **2004**, *108*, 3586–3592.
(24) Leary, R. H. Global Optimization on Funneling Landscapes. *J. Global Optim.* **2000**, *18*, 367–383.
(25) Takeuchi, H. Novel Method for Geometry Optimization of Molecular Clusters: Application to Benzene Clusters. *J. Chem. Inf. Model.* **2007**, *47*, 104–109.
(26) Pullan, W. J. Structural Prediction of Benzene Clusters Using a Genetic Algorithm. *J. Chem. Inf. Comput. Sci.* **1997**, *37*, 1189–1193.
(27) White, R. P.; Niesse, J. A.; Mayne, H. R. A Study of Genetic Algorithm Approaches to Global Geometry Optimization of Aromatic Hydrocarbon Microclusters. *J. Chem. Phys.* **1998**, *108*, 2208–2218.
(28) Easter, D. C. Low-Energy Structures of $(C_6H_6)_{13}$ as Determined by Low-Temperature Monte Carlo Simulations Using Several Potential Energy Surfaces. *J. Phys. Chem. A* **2003**, *107*, 2148–2159.
(29) Easter, D. C. Identification of a New C_3 Structure and Evidence for the Coexistence of Two $(Benzene)_{13}$ Cluster Isomers in Free Jet Expansions: A Monte Carlo Study. *J. Phys. Chem. A* **2003**, *107*, 7733–7742.
(30) Williams, D. E. Calculated Energy and Conformation of Clusters of Benzene Molecules and Their Relationship to Crystalline Benzene. *Acta Crystallogr., Sect. A: Fundam. Crystallogr.* **1980**, *36*, 715–723.
(31) van de Waal, B. W. Computed Structure of Small Benzene Clusters. *Chem. Phys. Lett.* **1986**, *123*, 69–72.
(32) Takeuchi, H. Geometry Optimization of Carbon Dioxide Clusters $(CO_2)_n$ for $4 \leq n \leq 40$. *J. Phys. Chem. A* **2008**, *112*, 7492–7497.
(33) Pillardy, J.; Olszewski, K. A.; Piela, L. Theoretically Predicted Lowest-Energy Structures of Water Clusters. *J. Mol. Struct.* **1992**, *270*, 277–285.
(34) Tsai, C. J.; Jordan, K. D. Theoretical Study of Small Water Clusters: Low-Energy Fused Cubic Structures for $(H_2O)_n$, $n = 8$, 12, 16, and 20. *J. Phys. Chem.* **1993**, *97*, 5208–5210.
(35) Sremaniak, L. S.; Perera, L.; Berkowitz, M. L. Cube to Cage Transitions in $(H_2O)_n$ ($n = 12$, 16, and 20). *J. Chem. Phys.* **1996**, *105*, 3715–3721.
(36) Niesse, J. A.; Mayne, H. R. Global Optimization of Atomic and Molecular Clusters Using the Space-Fixed Modified Genetic Algorithm Method. *J. Comput. Chem.* **1997**, *18*, 1233–1244.
(37) Wales, D. J.; Hodges, M. P. Global Minima of Water Clusters $(H_2O)_n$, $n \leq 21$, Described by an Empirical Potential. *Chem. Phys. Lett.* **1998**, *286*, 65–72.
(38) Qian, J.; Stöckelmann, E.; Hentschke, R. Global Potential Energy Minima of SPC/E Water Clusters without and with Induced Polarization Using a Genetic Algorithm. *J. Mol. Model.* **1999**, *5*, 281–286.
(39) Hartke, B. Global Geometry Optimization of Molecular Clusters: TIP4P Water. *Z. Phys. Chem.* **2000**, *214*, 1251–1264.
(40) Guimarães, F. F.; Belchior, J. C.; Johnston, R. L.; Roberts, C. Global Optimization Analysis of Water Clusters $(H_2O)_n$ ($11 \leq n \leq 13$) through a Genetic Evolutionary Approach. *J. Chem. Phys.* **2002**, *116*, 8327–8333.
(41) Kabrede, H.; Hentschke, R. Global Minima of Water Clusters $(H_2O)_N$, $N \leq 25$, Described by Three Empirical Potentials. *J. Phys. Chem. B* **2003**, *107*, 3914–3920.
(42) Hartke, B. Size-Dependent Transition from All-Surface to Interior-Molecule Structures in Pure Neutral Water Clusters. *Phys. Chem. Chem. Phys.* **2003**, *5*, 275–284.
(43) Kazimirski, J. K.; Buch, V. Search for Low Energy Structures of Water Clusters $(H_2O)_n$, $n = 20-22$, 48, 123, and 293. *J. Phys. Chem. A* **2003**, *107*, 9762–9775.
(44) James, T.; Wales, D. J.; Hernández-Rojas, J. Global Minima for Water Clusters $(H_2O)_n$, $n \leq 21$, Described by a Five-Site Empirical Potential. *Chem. Phys. Lett.* **2005**, *415*, 302–307.

(45) Kabrede, H. Using Vibrational Modes in the Search for Global Minima of Atomic and Molecular Clusters. *Chem. Phys. Lett.* **2006**, *430*, 336–339.
(46) Bandow, B.; Hartke, B. Larger Water Clusters with Edges and Corners on Their Way to Ice: Structural Trends Elucidated with an Improved Parallel Evolutionary Algorithm. *J. Phys. Chem. A* **2006**, *110*, 5809–5822.
(47) van der Avoird, A.; Szalewicz, K. Water Trimer Torsional Spectrum from Accurate Ab Initio and Semiempirical Potentials. *J. Chem. Phys.* **2008**, *128*, 014302-1–014302-8.
(48) Dahlke, E. E.; Olson, R. M.; Leverentz, H. R.; Truhlar, D. G. Assessment of the Accuracy of Density Functionals for Prediction of Relative Energies and Geometries of Low-Lying Isomers of Water Hexamers. *J. Phys. Chem. A* **2008**, *112*, 3976–3984.
(49) Fanourgakis, G. S.; Aprà, E.; Xantheas, S. S. High-Level Ab Initio Calculations for the Four Low-Lying Families of Minima of $(H_2O)_{20}$. I. Estimates of MP2/CBS Binding Energies and Comparison with Empirical Potentials. *J. Chem. Phys.* **2004**, *121*, 2655–2663.
(50) Lee, C.; Chen, H.; Fitzgerald, G. Chemical Bonding in Water Clusters. *J. Chem. Phys.* **1995**, *102*, 1266–1269.
(51) Tsai, C. J.; Jordan, K. D. Theoretical Study of the $(H_2O)_6$ Cluster. *Chem. Phys. Lett.* **1993**, *213*, 181–188.
(52) Bulusu, S.; Yoo, S.; Aprà, E.; Xantheas, S.; Zeng, X. C. Lowest-Energy Structures of Water Clusters $(H_2O)_{11}$ and $(H_2O)_{13}$. *J. Phys. Chem. A* **2006**, *110*, 11781–11784.
(53) McDonald, S.; Ojamäe, L.; Singer, S. J. Graph Theoretical Generation and Analysis of Hydrogen-Bonded Structures with Applications to the Neutral and Protonated Water Cube and Dodecahedral Clusters. *J. Phys. Chem. A* **1998**, *102*, 2824–2832.
(54) Lenz, A.; Ojamäe, L. Theoretical IR Spectra for Water Clusters $(H_2O)_n$ ($n = 6-22$, 28, 30) and Identification of Spectral Contributions from Different H-Bond Conformations in Gaseous and Liquid Water. *J. Phys. Chem. A* **2006**, *110*, 13388–13393.
(55) Maheshwary, S.; Patel, N.; Sathyamurthy, N.; Kulkarni, A. D.; Gadre, S. R. Structure and Stability of Water Clusters $(H_2O)_n$, $n = 8-20$: An Ab Initio Investigation. *J. Phys. Chem. A* **2001**, *105*, 10525–10537.
(56) Dauchez, M.; Peticolas, W. L.; Debelle, L; Alix, A. J. P. Ab Initio Calculations of Polyhedra Liquid Water. *Food Chem.* **2003**, *82*, 23–28.
(57) Lagutschenkov, A.; Fanourgakis, G. S.; Niedner-Schatteburg, G.; Xantheas, S. S. The Spectroscopic Signature of the "All-Surface" to "Internally Solvated" Structural Transition in Water Clusters in the $n = 17-21$ Size Regime. *J. Chem. Phys.* **2005**, *122*, 194310−1−194310−9.
(58) Goldman, N.; Saykally, R. J. Elucidating the Role of Many-Body Forces in Liquid Water I. Simulations of Water Clusters on the VRT(ASP-W) Potential Surfaces. *J. Chem. Phys.* **2004**, *120*, 4777–4789.
(59) Burnham, C. J.; Xantheas, S. S. Development of Transferable Interaction Potentials for Water. IV. A Flexible, All-Atom Polarizable Potential (TTM2-F) Based on Geometry Dependent Charges Derived from an Ab Initio Monomer Dipole Moment Surface. *J. Chem. Phys.* **2002**, *116*, 5115–5124.
(60) Fanourgakis, G. S.; Xantheas, S. S. Development of Transferable Interaction Potentials for Water. V. Extension of the Flexible, Polarizable, Thole-Type Model Potential (TTM3-F, v. 3.0) to Describe the Vibrational Spectra of Water Clusters and Liquid Water. *J. Chem. Phys.* **2008**, *128*, 074506-1–074506-11.
(61) Maeda, S.; Ohno, K. Structures of Water Octamers $(H_2O)_8$: Exploration on Ab Initio Potential Energy Surfaces by the Scaled Hypersphere Search Method. *J. Phys. Chem. A* **2007**, *111*, 4527–4534.
(62) Bukowski, R.; Szalewicz, K.; Groenenboom, G. C.; van der Avoird, A. Polarizable Interaction Potential for Water from Coupled Cluster Calculations. II. Applications to Dimer Spectra, Virial Coefficients, and Simulations of Liquid Water. *J. Chem. Phys.* **2008**, *128*, 094314-1–094314-20.
(63) Day, P. N.; Pachter, R.; Gordon, M. S.; Merrill, G. N. A Study of Water Clusters Using the Effective Fragment Potential and Monte Carlo Simulated Annealing. *J. Chem. Phys.* **2000**, *112*, 2063–2073.
(64) Tsoo, C.; Brooks, C. L., III. Cluster Structure Determination Using Gaussian Density Distribution Global Minimization Methods. *J. Chem. Phys.* **1994**, *101*, 6405–6411.
(65) Li, Z.; Laidig, K. E.; Daggett, V. Conformational Search Using a Molecular Dynamics-Minimization Procedure: Applications to Clusters of Coulombic Charges, Lennard-Jones Particles, and Waters. *J. Comput. Chem.* **1998**, *19*, 60–70.
(66) Dahlke, E. E.; Olson, R. M.; Leverentz, H. R.; Truhlar, D. G. Assessment of the Accuracy of Density Functionals for Prediction of Relative Energies and Geometries of Low-Lying Isomers of Water Hexamers. *J. Phys. Chem. A* **2008**, *112*, 3976–3984.
(67) Franken, K. A.; Jalaie, M.; Dykstra, C. E. Model Studies of Six-Membered Water Clusters. *Chem. Phys. Lett.* **1992**, *198*, 59–66.
(68) Wales, D. J.; Ohmine, I. Structure, Dynamics, and Thermodynamics of Model $(H_2O)_8$ and $(H_2O)_{20}$ Clusters. *J. Chem. Phys.* **1993**, *98*, 7245–7256.
(69) Wales, D. J.; Ohmine, I. Rearrangement of Model $(H_2O)_8$ and $(H_2O)_{20}$ Clusters. *J. Chem. Phys.* **1993**, *98*, 7257–7268.
(70) Hartke, B. Morphing Lennard-Jones Clusters to TIP4P Water Clusters: Why Do Water Clusters Look Like They Do. *Chem. Phys.* **2008**, *346*, 286–294.
(71) Jorgensen, W. L.; Chandrasekhar, J.; Madura, J. D.; Impey, R. W.; Klein, M. L. Comparison of Simple Potential Functions for Simulating Liquid Water. *J. Chem. Phys.* **1983**, *79*, 926–935.
(72) Liu, D. C.; Nocedal, J. On the Limited Memory BFGS Method for Large Scale Optimization. *Math. Prog.* **1989**, *45*, 503–528.
(73) Calvo, F.; Torchet, G.; de Feraudy, M.-F. Structural Transitions in Nitrogen Molecular Clusters: Experiment and Simulation. *J. Chem. Phys.* **1999**, *111*, 4650–4658.

CI800238W